Fault diagnosis in DC microgrids using nonlinear Kalman Filtering

Vassilios Siadimas
Research Associate
Industrial Systems Institute

Ευρωπαϊκή Ένωση
Ευρωπαϊκό Ταμείο
Περιφερειακής Ανάπτυξης

ΕΛΛΗΝΙΚΗ ΔΗΜΟΚΡΑΤΙΑ
ΥΠΟΥΡΓΕΙΟ
ΑΝΑΠΤΥΞΗΣ ΚΑΙ ΕΠΕΝΔΥΣΕΩΝ
ΕΙΔΙΚΗ ΓΡΑΜΜΑΤΕΙΑ ΔΙΑΡΘΡΩΤΙΚΩΝ ΠΡΟΓΡΑΜΜΑΤΩΝ
ΕΙΔΙΚΗ ΥΠΗΡΕΣΙΑ ΔΙΑΧΕΙΡΙΣΗΣ ΕΠΑνΕΚ

ΕΠΑνΕΚ 2014-2020
ΕΠΙΧΕΙΡΗΣΙΑΚΟ ΠΡΟΓΡΑΜΜΑ
ΑΝΤΑΓΩΝΙΣΤΙΚΟΤΗΤΑ
ΕΠΙΧΕΙΡΗΜΑΤΙΚΟΤΗΤΑ
ΚΑΙΝΟΤΟΜΙΑ

ΕΣΠΑ 2014-2020
ανάπτυξη - εργασία - αλληλεγγύη

Με τη συγχρηματοδότηση της Ελλάδας και της Ευρωπαϊκής Ένωσης

Fault diagnosis in DC Microgrids using nonlinear Kalman Filtering

G. Rigatos and N. Zervos

Unit of Industrial Automation
Industrial Systems Institute
26504, Rion Patras, Greece
grigat@ieee.org

M. Abbaszadeh

GE Global Research
General Electric
Niskayuna, 12309, NY, USA
masouda@ualberta.net

P. Siano

Dept of Industrial Eng.
University of Salerno
84084, Fisciano, Italy
psiano@unisa.it

V.Siadimas

Dept of Electrical Eng.
University of Patras
26504, Rion Patras, Greece
siadimasv@gmail.com

D. Serpanos

Dept of Electrical Eng.
University of Patras
26504, Rion Patras, Greece
serpanos@isi,gr

1 . Introduction

● To solve the **condition monitoring problem** for **DC microgrids** the article proposes **robust Kalman Filtering** in the form of the **H-infinity Kalman Filter**.

● To extend the use of the **H-infinity Kalman Filter** to nonlinear dynamic models of the electricity grid it is proposed to apply **approximate linearization** that relies on first-order **Taylor series expansion** and on the computation of the associated Jacobian matrices.

● The linearization process takes place around a **time-varying operating point** which is re-computed **at each time-step** of the condition monitoring algorithm. The filter emulates the functioning of the DC microgrid in the fault-free and cyber-attack-free case.

● At a next stage, the **residuals' sequence** is generated by subtracting the outputs of the filter from the real outputs of the DC microgrid. It is proven that the **stochastic variable (statistical test)** which is defined by the sum of the squares of the residuals' vectors weighted by the inverse of the associated covariance matrix, follows the χ^2 **distribution**.

● The **confidence intervals of the** χ^2 **distribution** define ranges about the normal functioning of the DC microgrid. When the value of the previously noted **statistical test** falls within these confidence intervals, one can infer that the DC microgrid has not been affected by any type of fault or cyber-attack.

● Finally, by applying the **statistical condition monitoring method** into subspaces of the DC microgrid's state-space description, **fault and cyber-attack isolation** can be also performed.

2 . Dynamic model of the DC microgrid

An indicative **DC microgrid** which can supply with power an **industrial unit** is shown in the following diagram (Fig. 1)

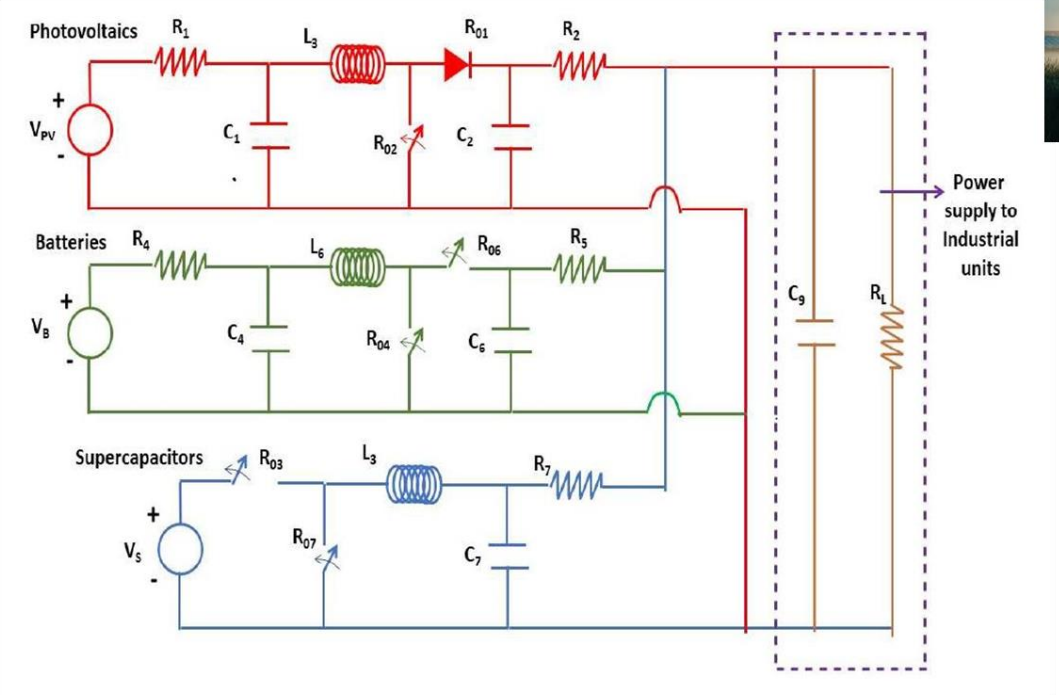

Fig. 1: Use of a DC microgrid that comprises photovoltaics, batteries and supercapacitors to provide electric power to industrial units

2. Dynamic model of the DC microgrid

The **dynamic model of the DC microgrid** is described by the following set of equations:

$$\dot{x}_1 = -\frac{1}{R_1C_1}x_1 - \frac{1}{C_1}x_3 + \frac{1}{R_1C_1}V_{PV} \tag{1}$$

$$\dot{x}_2 = -\frac{1}{R_2C_2}x_2 - \frac{1}{C_2}x_3 - \frac{1}{C_2}x_3u_1 + \frac{1}{R_2C_2}x_9 \tag{2}$$

$$\dot{x}_3 = \frac{1}{L_3}(x_1 - x_2 - R_{o_1}x_3) + \frac{1}{L_3}(x_2 + (R_{o_1} - R_{o_2})x_3)u_1 \tag{3}$$

$$\dot{x}_4 = -\frac{1}{R_4C_4}x_4 - \frac{1}{C_4}x_6 + \frac{1}{R_4C_4}V_B \tag{4}$$

$$\dot{x}_5 = -\frac{1}{R_5C_5}x_5 + \frac{1}{C_5}x_6 + \frac{1}{R_5C_5}x_9 - \frac{1}{C_5}x_6u_2 \tag{5}$$

$$\dot{x}_6 = \frac{1}{L_6}x_4 - \frac{1}{L_6}x_5 - \frac{R_{o_4}}{L_6} + \frac{1}{L_6}x_5u_2 \tag{6}$$

$$\dot{x}_7 = -\frac{1}{R_7C_7}x_7 + \frac{1}{C_7}x_8 + \frac{1}{R_7C_7}x_9 \tag{7}$$

$$\dot{x}_8 = \frac{1}{L_8}V_su_3 - \frac{R_{08}}{L_8}x_8 - \frac{1}{L_8}x_7 \tag{8}$$

$$\dot{x}_9 = \frac{1}{C_9}\left(\frac{x_2 - x_9}{R_2} + \frac{x_5 - x_9}{R_5} + \frac{x_7 - x_9}{R_7} - x_9\frac{1}{R_L}\right) \tag{9}$$

2 . Dynamic model of the DC microgrid

The **state variables of the dynamic model** of the DC microgrid are defined as follows

x_1 is voltage V_{c1} at capacitor C_1

x_2 is voltage V_{c2} at capacitor C_2

x_3 is current i_{L3} at the inductor L_3

x_4 is voltage V_{C4} at the capacitor C_4

x_5 is voltage V_{C5} at the capacitor C_5

x_6 is current i_{L6} at the inductor L_6

x_7 is voltage V_{C7} at the capacitor C_7

x_8 is current i_{L8} at the inductor L_8

x_9 is voltage V_{C9} at the capacitor C_9

Control is implemented with the use of the **Pulse Width Modulation (PWM)** approach.

The **control inputs of the dynamic model** of the DC microgrid are:

u_1 which stands for the duty cycle of the switch at the PV circuit,

u_2 which is the duty cycle of the switch at the battery circuit

u_3 which is the duty cycle of the switch at the supercapacitor circuit.

2 . Dynamic model of the DC microgrid

Next, the **state-space model of the DC microgrid** is written in the following matrix form

$$\begin{pmatrix} \dot{x}_1 \\ \dot{x}_2 \\ \dot{x}_3 \\ \dot{x}_4 \\ \dot{x}_5 \\ \dot{x}_6 \\ \dot{x}_7 \\ \dot{x}_8 \\ \dot{x}_9 \end{pmatrix} = \begin{pmatrix} -\frac{1}{R_1C_1}x_1 - \frac{1}{C_1}x_3 + \frac{1}{R_1C_1}V_{PV} \\ -\frac{1}{R_2C_2}x_2 - \frac{1}{C_2}x_3 + \frac{1}{R_2C_2}x_9 \\ -\frac{1}{R_4C_4}x_4 - \frac{1}{C_4}x_6 + \frac{1}{R_4C_4}V_B \\ \frac{1}{L_3}(x_1 - x_2 - R_{o_1}x_3) + \frac{1}{L_3}x_2 \\ -\frac{1}{R_5C_5}x_5 + \frac{1}{C_5}x_6 + \frac{1}{R_5C_5}x_9 \\ \frac{1}{L_6}x_4 - \frac{1}{L_6}x_5 - \frac{R_{o_4}}{L_6} \\ -\frac{1}{R_7C_7}x_7 + \frac{1}{C_7}x_8 + \frac{1}{R_7C_7}x_9 \\ -\frac{R_{08}}{L_8}x_8 - \frac{1}{L_8}x_7 \\ \frac{1}{C_9}\left(\frac{x_2-x_9}{R_2} + \frac{x_5-x_9}{R_5} + \frac{x_7-x_9}{R_7} - x_9\frac{1}{R_L}\right) \end{pmatrix} + \begin{pmatrix} 0 & 0 & 0 \\ -\frac{1}{C_2}x_3 & 0 & 0 \\ (R_{o_1} - R_{o_2})x_3 & 0 & 0 \\ 0 & 0 & 0 \\ 0 & -\frac{1}{C_5}x_6 & 0 \\ 0 & +\frac{1}{L_6}x_5 & 0 \\ 0 & 0 & 0 \\ 0 & 0 & \frac{1}{L_8}V_s \\ 0 & 0 & 0 \end{pmatrix} \begin{pmatrix} u_1 \\ u_2 \\ u_3 \end{pmatrix} \quad (10)$$

Consequently, the state-space model of DC microgrid is written in the following **affine-in-the-input state space form**

$$\dot{x} = f(x) + g(x)u \quad (11)$$

where $x \in R^{9\times1}$, $u \in R^{3\times1}$, $f(x) \in R^{9\times1}$ and $g(x) \in R^{9\times3}$

3. Approximate linearization of the DC microgrid

The **dynamic model of the DC microgrid** undergoes **approximate linearization** around a temporary operating point (x*,u*),

x* is the present value of the system's state vector
u* is the last value of the control inputs vector

The **operating point** is updated at each iteration of the control method. The linearization procedure makes use of first-order **Taylor series expansion** and relies on the computation of the associated **Jacobian matrices.**

This gives:

$$\dot{x} = Ax + Bu + \tilde{d} \qquad (12)$$

$\bar{d}$ is the modelling error due to **truncation of higher-order terms** in Taylor series expansion

Matrices A and B are given (13)

$$A = \nabla_x[f(x) + g_1(x)u_1 + g_2(x)u_2 + g_3(x)u_3] \mid_{(x^*,u^*)} \Rightarrow$$

$$A = \nabla_x[f(x)] \mid_{(x^*,u^*)} + \nabla_x[g_1(x)]u_1 \mid_{(x^*,u^*)} + \nabla_x[g_2(x)]u_2 \mid_{(x^*,u^*)} + \nabla_x[g_3(x)]u_3 \mid_{(x^*,u^*)}$$

$$B = \nabla_x[f(x) + g_1(x)u_1 + g_2(x)u_2 + g_3(x)u_3] \mid_{(x^*,u^*)} \Rightarrow B = g(x) \mid_{(x^*,u^*)} \qquad (14)$$

3. Approximate linearization of the DC microgrid

Computation of the **Jacobian matrix** $\nabla_x[f(x)]\mid_{(x^*,u^*)}$

$$\nabla_x[f(x)]\mid_{(x^*,u^*)}=\begin{pmatrix} -\frac{1}{R_1C_1} & 0 & -\frac{1}{C_3} & 0 & 0 & 0 & 0 & 0 & 0 \\ 0 & -\frac{1}{R_2C_2} & \frac{1}{C_3} & 0 & 0 & 0 & 0 & 0 & 0 \\ \frac{1}{L_3} & -\frac{1}{L_3} & -\frac{R_{o1}}{L_3} & 0 & 0 & 0 & 0 & 0 & 0 \\ 0 & 0 & 0 & -\frac{1}{R_4C_4} & 0 & -\frac{1}{C_4} & 0 & 0 & 0 \\ 0 & 0 & 0 & 0 & -\frac{1}{R_5C_5} & -\frac{1}{C_5} & 0 & 0 & \frac{1}{R_5c_5} \\ 0 & 0 & 0 & \frac{1}{L_6} & -\frac{1}{L_6} & -\frac{R_{o4}}{L_6} & 0 & 0 & 0 \\ 0 & 0 & 0 & 0 & 0 & 0 & -\frac{1}{R_7C_7} & \frac{1}{C_7} & \frac{1}{R_7C_7} \\ 0 & 0 & 0 & 0 & 0 & 0 & -\frac{1}{L_8} & -\frac{R_{o8}}{L_8} & 0 \\ 0 & \frac{1}{C_9R_2} & 0 & 0 & \frac{1}{C_9R_5} & 0 & \frac{1}{C_9R_7} & 0 & \frac{\partial f_9}{\partial x_9} \end{pmatrix} \quad (15)$$

where $\frac{\partial f_9}{\partial x_9}=-\frac{1}{C_9R_2}-\frac{1}{C_9R_5}-\frac{1}{C_9R_7}-\frac{1}{R_L}$

Computation of the **Jacobian matrix** $\nabla_x[g_1(x)]\mid_{(x^*,u^*)}$

$$\nabla_x g_1[x)]\mid_{(x^*,u^*)}=\begin{pmatrix} 0 & 0 & 0 & 0 & 0 & 0 & 0 & 0 & 0 \\ 0 & 0 & -\frac{1}{C_2} & 0 & 0 & 0 & 0 & 0 & 0 \\ 0 & \frac{1}{L_3} & \frac{R_{o1}-R_{o2}}{L_3} & 0 & 0 & 0 & 0 & 0 & 0 \\ 0 & 0 & 0 & 0 & 0 & 0 & 0 & 0 & 0 \\ 0 & 0 & 0 & 0 & 0 & 0 & 0 & 0 & 0 \\ 0 & 0 & 0 & 0 & 0 & 0 & 0 & 0 & 0 \\ 0 & 0 & 0 & 0 & 0 & 0 & 0 & 0 & 0 \\ 0 & 0 & 0 & 0 & 0 & 0 & 0 & 0 & 0 \\ 0 & 0 & 0 & 0 & 0 & 0 & 0 & 0 & 0 \end{pmatrix} \quad (16)$$

3. Approximate linearization of the DC microgrid

Computation of the **Jacobian matrix** $\nabla_x[g_2(x)]\mid_{(x^*,u^*)}$

$$\nabla_x g_2[x)]\mid_{(x^*,u^*)}=\begin{pmatrix} 0&0&0&0&0&0&0&0&0\\ 0&0&0&0&0&0&0&0&0\\ 0&0&0&0&0&0&0&0&0\\ 0&0&0&0&0&-\frac{1}{C_5}&0&0&0\\ 0&0&0&0&\frac{1}{C_6}&0&0&0&0\\ 0&0&0&0&0&0&0&0&0\\ 0&0&0&0&0&0&0&0&0\\ 0&0&0&0&0&0&0&0&0\\ 0&0&0&0&0&0&0&0&0 \end{pmatrix} \quad (17)$$

Computation of the **Jacobian matrix** $\nabla_x[g_3(x)]\mid_{(x^*,u^*)}$: $\nabla_x g_2[x)]\mid_{(x^*,u^*)}=0_{9\times 9}$.

For the DC microgrid a stabilizing (H-infinity) feedback controller is

$$u(t)=-Kx(t) \quad (18)$$

with $K=\frac{1}{r}B^TP$ where P is a positive definite symmetric matrix which is obtained from the solution of the **Riccati equation**

$$A^TP+PA+Q-P(\frac{2}{r}BB^T-\frac{1}{\rho^2}LL^T)P=0 \quad (19)$$

where Q is a positive semi-definite symmetric matrix.

4 The H-infinity Kalman Filter

The **H-infinity KF** is an optimal **state estimator under model uncertainty** and perturbations and thus its use under the variable operating conditions of DC microgrid is advantageous.

The H-infinity KF is addressed to linear systems and to use it in the DC microgrid model, the previously analyzed **approximate linearization**. was applied

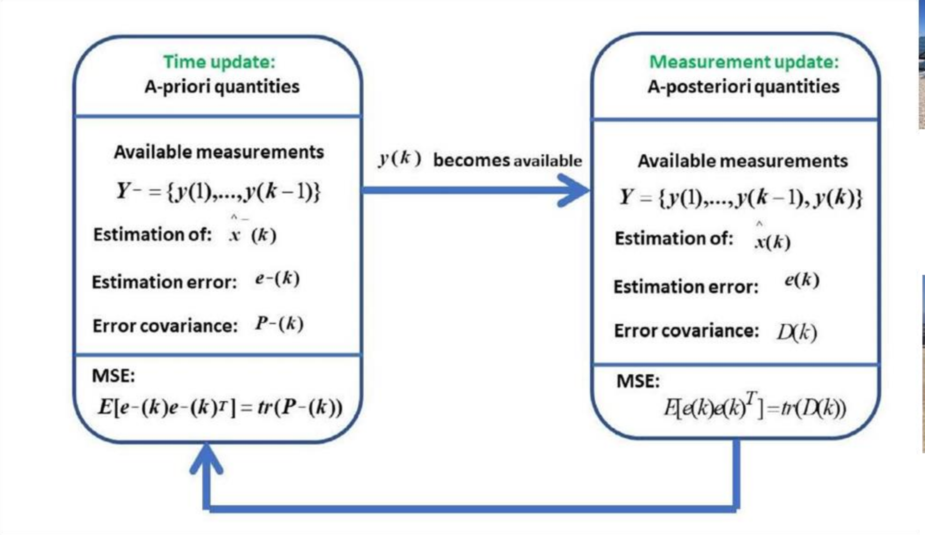

Fig. 2 Diagram of the H-infinity Kalman Filter comprising a time-update part and a measurement update part

4 The H-infinity Kalman Filter

- By comparing the filter's output against the real outputs of the DC microgrid, the **residuals sequence** is generated, which in turn can be used for fault diagnosis purposes.

- The **recursion of the H-infinity Kalman Filter**, for the **DC microgrid**, can be formulated in terms of a measurement update and a time update part

Measurement update

$$
\begin{aligned}
D(k) &= [I - \theta W(k)P^{-}(k) + C^{T}(k)R(k)^{-1}C(k)P^{-}(k)]^{-1}\\
K(k) &= P^{-}(k)D(k)C^{T}(k)R(k)^{-1}\\
\hat{x}(k) &= \hat{x}^{-}(k) + K(k)[y(k) - C\hat{x}^{-}(k)]
\end{aligned} \quad (20)
$$

Time update

$$
\begin{aligned}
\hat{x}^{-}(k+1) &= A(k)x(k) + B(k)u(k)\\
P^{-}(k+1) &= A(k)P^{-}(k)D(k)A^{T}(k) + Q(k)
\end{aligned} \quad (21)
$$

where it is assumed that parameter θ is sufficiently small to assure that **matrix**

$$P^{-1}(k) - \theta W(k) + C^{T}(k)R(k)^{-1}C(k)$$

is **positive definite**

4 The H-infinity Kalman Filter

The **H-infinity Kalman Filter exhibits advantages** against other nonlinear filters

EKF is not robust against linearization errors and measurement noise.
UKF methods are not of proven convergence and stability.
PF demands high computation power and has slow convergence

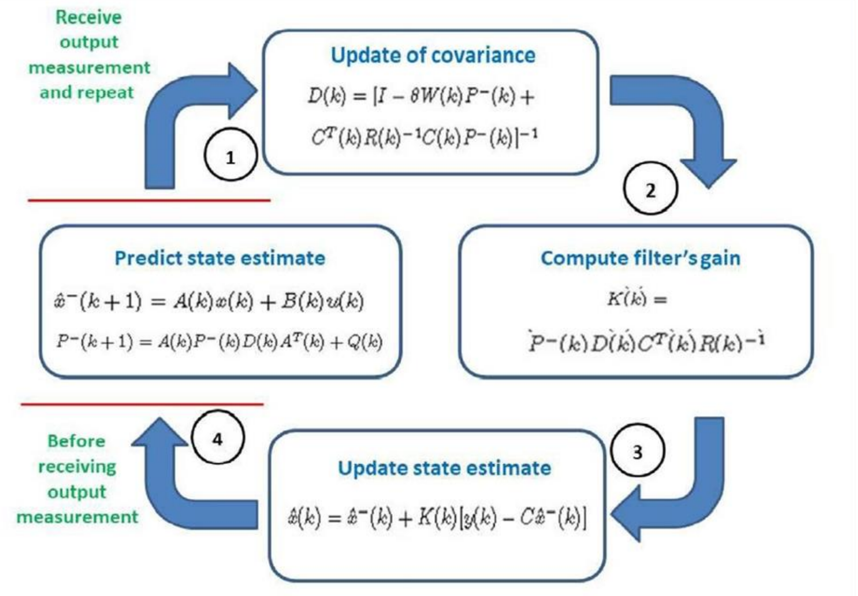

Fig. 3 The sequence of computations that constitute the H-infinity Kalman Filter.

Research & Innovation Information Technologies

5. Statistical fault diagnosis with the use of the Kalman Filter

The **residuals' sequence**, that is the differences between (i) the **real outputs of the DC microgrid** and (ii) the **outputs estimated by the Kalman Filter** is used for concluding the appearance of a fault or cyberattack

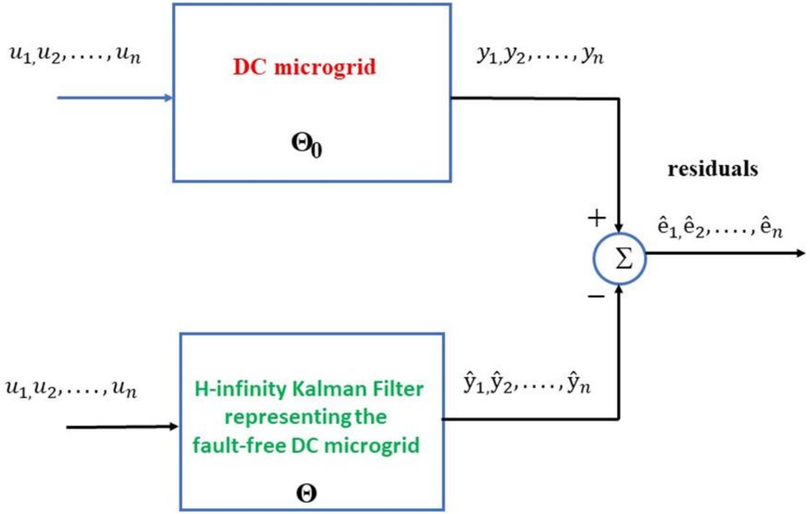

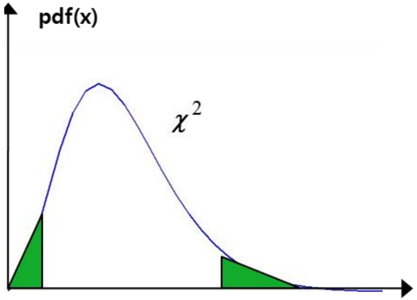

Fig. 4 Residuals generation with the use of the H-infinity Kalman Filter

5. Statistical fault diagnosis with the use of the Kalman Filter

The **residuals' sequence** e_k is a **zero-mean Gaussian white-noise process** with covariance E_k

The **following normalized error square (NES) is defined**

$$\epsilon_k = e_k^T E_k^{-1} e_k \quad (22)$$

The **normalized error square follows a χ^2 distribution**. An appropriate test for the normalized error sum is to numerically show that the following condition is met within a level of confidence

$$E\{\epsilon_k\} = m \quad (23)$$

This can be achieved using **statistical hypothesis testing**, which is associated with **confidence intervals**. A 95% confidence interval is frequently applied, which is specified using 100(1−a) with a = 0.05. Actually, a two-sided probability region is considered cutting-off two end tails of 2.5% each. For M runs the **normalized error square** that is obtained is given by

$$\bar{\epsilon}_k = \frac{1}{M}\sum_{i=1}^{M}\epsilon_k(i) = \frac{1}{M}\sum_{i=1}^{M}e_k^T(i)E_k^{-1}(i)e_k(i) \quad (24)$$

5. Statistical fault diagnosis with the use of the Kalman Filter

Then $M\bar{\epsilon}_k$ will follow a **χ^2 density with Mm degrees of freedom**. This condition can be checked using a χ^2 test. The hypothesis holds, if the following condition is satisfied

$$\bar{\epsilon}_k \in [\zeta_1, \zeta_2] \quad (25)$$

where ζ_1 and ζ_2 are derived from the tail probabilities of the χ^2 density.

By applying the **statistical test into subspaces of the state-space description** of the DC microgrid, it is also possible to find out the specific component that has been subject to a fault or cyberattack

Starting from the **initial state vector of dimension** n one can perform the fault diagnosis test with **sub-vectors of dimension** k, where each sub-vector comprises k out of n state vector elements of the system.

The total number of tests is

$$\binom{n}{k} = \frac{n}{k!(n-k)!} \quad (26)$$

The **tests that exhibit the highest score** designate also the parts of the power system which are more likely to be subjected to fault or cyber-attack

6. Simulation tests

- Considering **n = 9 measurable outputs** for the DC microgrid, to conclude the normal functioning of the power unit, the previously analyzed **statistical test should** take a value that is very close to the **mean value of χ^2 distribution, that is 9**.

- To perform the faults detection and isolation tests with the previously analyzed χ^2 statistical criterion one can define the **output measurements vector $y_m = [x_1 \ldots x_9]$** where x_i i=1,…,9 are the state vector elements of the DC microgrid

- The dimension of the outputs measurements vector is n=9. Considering that the number of output vector samples is M=2000 and using a **98% confidence interval** for the χ^2 distribution the **fault thresholds can be as L=8.85 and U=9.15.**

- By **applying the statistical test into subspaces** of the state-space model defined by state vector elements which are related exclusively with the PV power system, the supercapacitor and the battery, one can also perform **fault isolation** for the components of the DC microgrid

- The simulation experiments confirm that, as long as the value of the statistical test falls within these **confidence intervals**, it can be concluded that the functioning of the DC microgrid is normal. On the other side, when the **above noted upper or lower bound are exceeded** it can be concluded that the system has been **subject to a failure** and an alarm can be launched.

6. Simulation tests

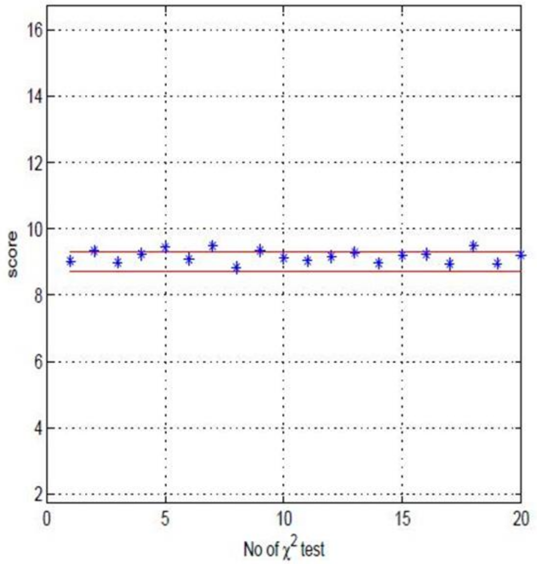

Fig. 5(a) Values of successive χ^2 tests when no fault exists at the DC microgrid

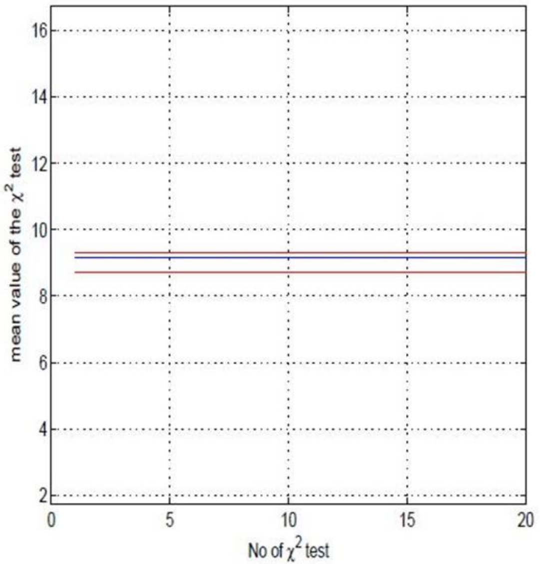

Fig. 5(b) Mean value of the χ^2 tests when no fault exists at the DC microgrid

6. Simulation tests

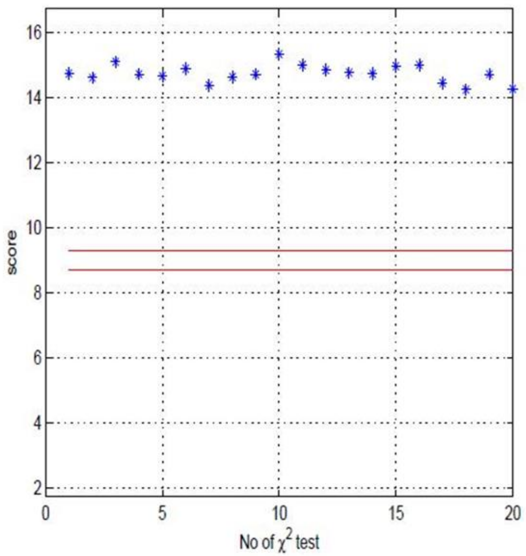

Fig. 6(a) Values of successive χ^2 tests when a fault affects control input (duty cycle) u_1

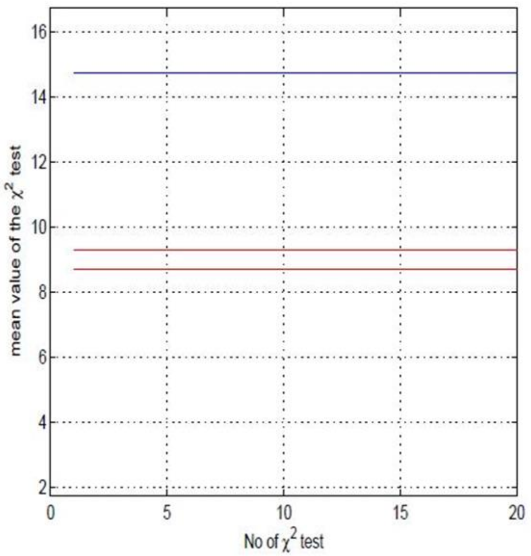

Fig 6(b) Mean value of the χ^2 tests when a fault affects control input (duty cycle) u_1

6. Simulation tests

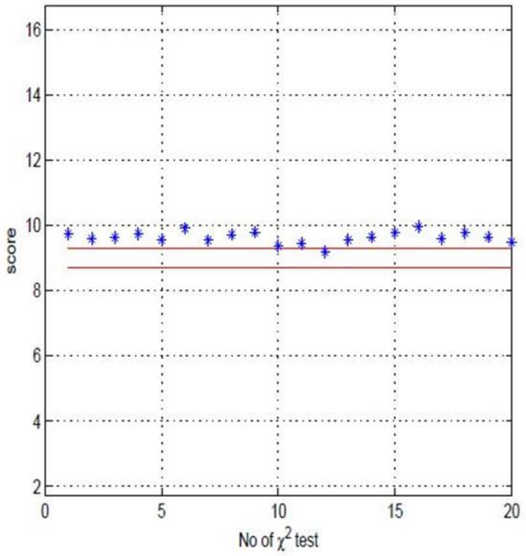

Fig. 7(a) Values of successive χ^2 tests when a fault affects control input (duty cycle) u_2

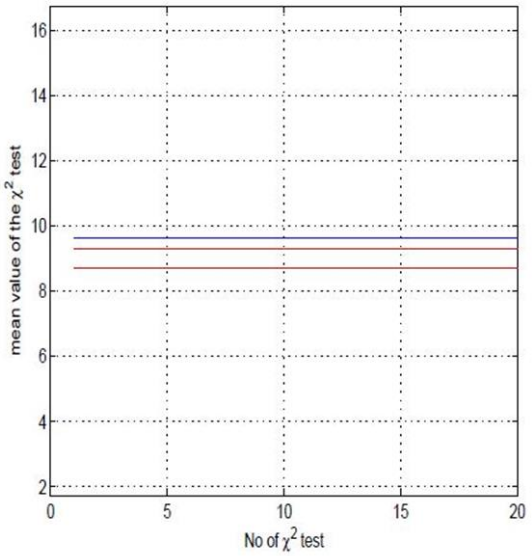

Fig. 7(b) Mean value of the χ^2 tests when a fault affects control input (duty cycle) u_2

6. Simulation tests

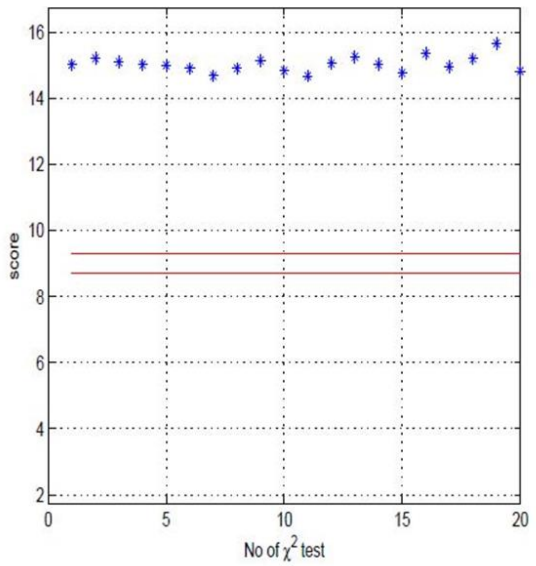

Fig. 8(a) Values of successive χ^2 tests when a fault affects control input (duty cycle) u_3

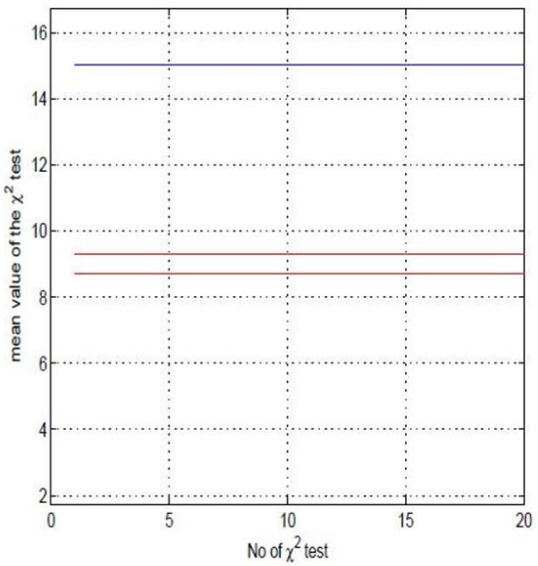

Fig. 8(b) Mean value of the χ^2 tests when a fault affects control input (duty cycle) u_3

ATHENA Research & Innovation Information Technologies

6. Simulation tests

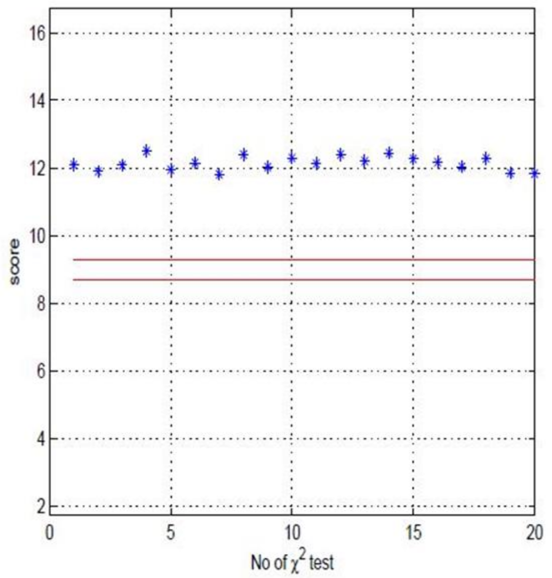

Fig. 9(a) Values of successive χ^2 tests when a fault affects the voltage source V_{PV}

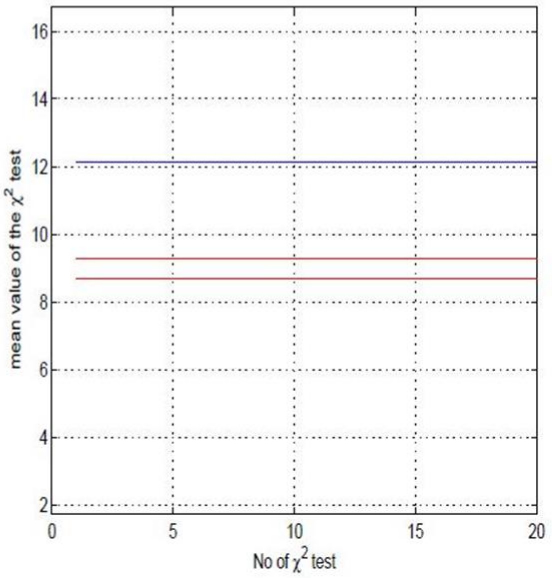

Fig. 9(b) Mean value of the χ^2 tests when a fault affects the voltage source V_{PV}

6. Simulation tests

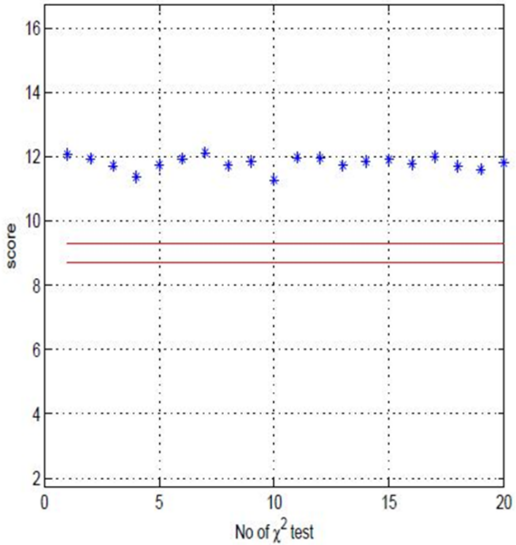

Fig. 10(a) Values of successive χ^2 tests when a fault affects the voltage source V_b

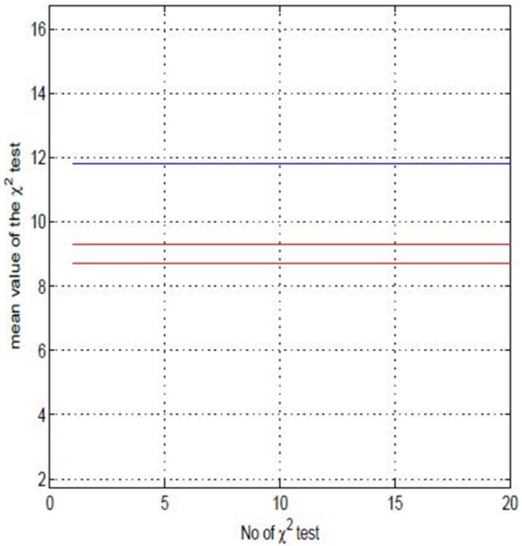

Fig. 10(b) Mean value of the χ^2 tests when a fault affects the voltage source V_b

6. Simulation tests

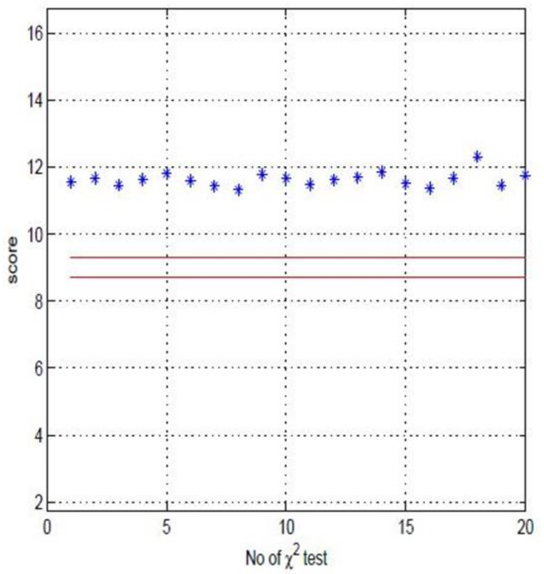

Fig. 11(a) Values of successive χ^2 tests when a fault affects the voltage source V_{sc}

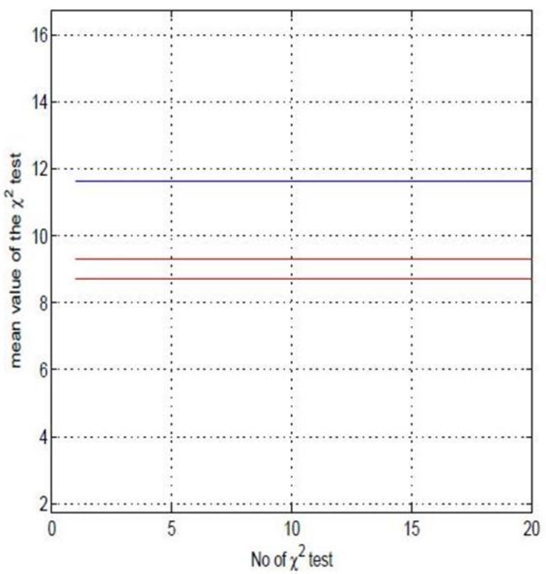

Fig. 11(b) Mean value of the χ^2 tests when a fault affects the voltage source V_{sc}

7 . Conclusions

- Due to being exposed to variable and harsh operating conditions, **DC microgrids undergo failures**.

- Furthermore, when **DC microgrids function as part of networked control schemes** they become exposed to **cyber-attacks** targeting their control and data acquisition software.

- It is important to accomplish **early fault detection** and **incipient failure diagnosis** for DC microgrids, so as to avoid excessive damage of this equipment and to take action for its repair.

- This research work has introduced a novel **fault diagnosis method for DC microgrids** which relies on the use of a **robust state estimator**, that is the **H-infinity Kalman Filter.**

- To enable the use of the H-infinity Kalman Filter in a nonlinear model, the related **state-space description undergoes linearization** through **Taylor series** expansion.

- The linearization is performed around a **temporary operating point** which is recomputed at **each time-step** of the condition monitoring method.

The H-infinity Kalman Filter **emulates the functioning of the DC microgrid in the fault-free case**.

ATHENA Research & Innovation Information Technologies

7. Conclusions

- By comparing the output estimates provided by the filter against the real outputs of the DC microgrid, a **residual vectors sequence** is generated.

- The **sum of the squares of the residuals vectors**, weighted by the inverse of the associated covariance matrix was shown to be a **stochastic variable (statistical test)** which follows the **χ^2 distribution**.

- The **confidence intervals of the χ^2 distribution** have allowed to define certainty levels for finding the system in the fault-free condition.

- As long as the value of the previously noted stochastic variable falls within these **confidence intervals** one can conclude in an almost infallible manner (e.g. with certainty of the order of 96% or 98%) that **the DC microgrid functions properly.**

- On the other side, when the value of **the stochastic variable exceeds the confidence interval** it can be inferred that the DC microgrid is in a **faulty state** and an alarm can be launched.

- Additionally, by carrying out the statistical test into **subspaces of the DC microgrid's state-space description** one can achieve **fault isolation**.

Thank you for your attention

VIRTUAL EVENT

Ημέρες Δράσης

23-24-25 ΙΟΥΝΙΟΥ 2021

Ευχαριστώ!

ATHENA Research & Innovation Information Technologies

Contact Details

Address Industrial Systems Institute
26504, Rion Patras, Greece

Tel +30-2610-910297

Email grigat@ieee.org
siadimasv@gmail.com